atmosphere

MDPI

Article

Automatic Analysis of Trough Lines Based on Curvature Tracing

Qian Li [1,†], Yan Huang [1,2,*,†], Yin Fan [1], Shaoen Tang [1] and Yuntao Hu [1]

[1] College of Meteorology and Oceanography, National University of Defense Technology, Nanjing 210001, China; public_liqian@163.com (Q.L.); a13913933999@163.com (Y.F.); public_tangshaoen@163.com (S.T.); desperadold@163.com (Y.H.)

[2] 92001 PLA troops, Qingdao 266011, China

* Correspondence: huangyan11212062@163.com; Tel.: +86-25-8083-0644

† These authors contributed equally to this work.

Received: 7 November 2017; Accepted: 12 February 2018; Published: 1 March 2018

Abstract: To solve the problems that arise in traditional automatic methods for trough line analysis with regard to low processing efficiency and analytical accuracy, an automatic method for trough line analysis was proposed in this study, comprising the following steps. Firstly, the curvature of contour lines was calculated using geopotential height field data to extract tracing start points, and candidate and non-candidate trough points were classified and recognized based on their curvature and relative positions. Afterwards, among the candidates, the eligible trough points were connected from tracing start point. Finally, the automatically analyzed trough lines were obtained after some post-processing steps. The experimental results indicate that the method is able to effectively identify meteorological trough lines, and that its performance is superior to some previous analysis methods of trough line in terms of analytical accuracy and processing speed.

Keywords: trough lines; automatic analysis; geopotential height field; curvature tracing

1. Introduction

With the increase in forecasting requirements in the meteorological field, forecasters need to collect and process large quantities of observational data and numerical simulation data, which creates a great challenge for the accurate and efficient analysis of massive volumes of information and the completion of forecasting work. Therefore, various countries are vigorously developing synoptic automatic analysis systems. To date, several synoptic automatic analysis systems have realized the automatic analysis of contours and streamlines, including the Meteorological Information Comprehensive Analysis and Process System (MICAPS) [1,2], the US civilian Advanced Weather Interactive Processing System (AWIPS) [3,4] and so on. However, due to the complexity of high-altitude weather systems and some meteorological constraints, the analysis of trough lines are still mainly accomplished manually.

In terms of the geopotential height field, a trough is an elongated region in low-pressure areas, and is generally called a trough line on weather charts [5]. By definition, trough lines are lines that connect the points with the highest contour curvature, and the recognition of trough lines has important guiding significance in weather condition determination and disaster weather forecasting, which makes trough lines analysis a significant problem. It can be seen that implementing the automatic analysis and visualization of trough lines by means of computer technology [6] can not only improve the effectiveness of weather chart analysis, but can also allow forecasters to judge the weather system structure and evolution trends of trough lines more objectively. Therefore, the study of automatic analysis of trough lines has important practical value.

Nevertheless, the automatic analysis of trough lines has not been a focus of researchers. In the existing body of research, Huang et al. [7,8] identified troughs' characteristics through the establishment

of a relational spatial aggregation framework, and extracted trough lines by connecting the points of the largest contour curvature. Hu et al. [9] utilized the vector rotation tracing method to conduct a contour analysis and determined the central location of synoptic systems, such as troughs and ridges, through the relationship between the characteristic points and their adjacent isobaric lines. Wong et al. [10] identified low-pressure regions by defining a fitness function based on a genetic algorithm, and the adjacent curvature segment of the isobaric line was regarded as the characteristic trough line. Moreover, Mou et al. [11] first identified the isobaric line in pressure field data through the edge detection algorithm and then analyzed the trough points and trough lines based on the ant colony algorithm. Based on the Douglas-Peucker algorithm, Dai et al. [12] extracted the curvature characteristic points from an isobaric line as trough points, and the trough point connection rule was established based on the topological structure of an isobaric line in order to attain analysis results of a trough line. Although the methods above can essentially accomplish the automatic analysis of trough and ridge lines, there are some drawbacks to these methods: (1) the extraction of the contour lines, which is a necessary step in these methods, is still time-consuming and reduces the efficiency of these methods; (2) the accuracy of the trough lines analyzed is affected because the extracted contours are susceptible to distortion, and deviation is introduced when the curvature of the sampling points of the contours are calculated.

Similar to the analysis of trough lines, geography researchers have also presented some methods to identify valleys (ridges) with terrain data. For example, Ohtake et al. [13] firstly used triangular mesh to segment the set of contours, and estimated the higher-order derivative of contours with implicit surface fitting and finite difference methods, and ultimately determined the valley (ridge) lines by the curvature extremes; however, in this method, the contour lines still need to be analyzed in advance. In addition, Pang [14] defined a principal curvature algorithm to extract the valley (ridge) line from the point set model. In general, the methods above do not consider meteorological constraints, such as the balance of air volume and air pressure, so they can't deal with the problem of noise points. Furthermore, their computing cost is expensive for the contour extraction or the calculation of principal curvature.

This paper proposes an automatic analysis method for trough lines based on curvature tracing. To our knowledge, there are, as yet, no methodologies for the automatic analysis of trough lines based on curvature tracing. Compared to the existing methods, our proposed method is able to improve the processing efficiency and accuracy of the extraction of trough lines by avoiding the analysis of contours. First of all, the curvature values of the grid points are calculates directly from the geopotential height field data, and the candidate trough points are extracted based on the classification of grid points based on the curvature, from among which the reasonable trough points are selected for the tracing and connecting of the trough lines.

2. Proposed Methodology

The method uses an input field given on gridded data. Firstly, geopotential height data are used to calculate the curvature value at each grid point, and the grid points are then classified to extract the tracing starting point and the candidate trough points (i.e., the key points in the process of trough line tracing). Subsequently, the reasonable trough points are traced and connected to obtain the raw trough lines on the basis of a number of relevant constraints. Finally, post-processing steps are indispensable, including trough line noise removal and curve smoothing.

2.1. Curvature Calculation

As presented as a principle of meteorology [15], vorticity represents the degree and direction of rotation at a certain point in the wind field. The vorticity calculation in the natural coordinate system is as follows:

$$\xi_g = V\frac{\partial \alpha}{\partial s} - \frac{\partial V}{\partial n} \quad (1)$$

where α is the wind direction at that point, V is the wind speed magnitude, s represents the wind speed direction, and n is the normal vector of s.

Since the trough line often occurs in the upper atmosphere, and in high-latitude areas, the genuine wind in the upper atmosphere is very close to the geostrophic wind (the horizontal uniform linear motion of air in the free atmosphere).Therefore, assuming that geostrophic wind can replace true wind, then Equation (1) can be written as:

$$\xi_g = V_g K - \frac{\partial V_g}{\partial n} \tag{2}$$

where V_g is geostrophic wind speed, K is the curvature of the streamline, and $V_g K$ is the curvature vorticity, which represents the vorticity caused by the bending of the streamline (contour). The larger the wind speed, the larger the vorticity. The term $-\frac{\partial V_g}{\partial n}$ is the shear vorticity. In the Northern Hemisphere, when cyclonic shear is present, the vorticity is positive, and in case of anticyclonic shear, the vorticity is negative. Mathematically, the curvature value C of the contour at a certain point is equivalent to the value of K in Equation (2). Combined with Equation (1), we obtain:

$$C = K = \frac{\partial \alpha_g}{\partial s_g} \tag{3}$$

where α_g is the wind angle of the geostrophic wind at that point, and s_g is the direction of the geostrophic wind. Thus, to calculate the curvature value C, it is necessary to use the geopotential height data to calculate the wind angle α_g of the geostrophic wind at each point on the isobaric surface. In the movement of geostrophic wind, only the horizontal pressure gradient force and the Coriolis force are acting, which indicates that the magnitude of the geostrophic wind is proportional to the horizontal pressure gradient and negatively proportional to the sine of the latitude. This can be shown in component form as:

$$u_g = -\frac{1}{f}\frac{\partial \Phi}{\partial y}\ v_g = \frac{1}{f}\frac{\partial \Phi}{\partial x} \tag{4}$$

where u_g and v_g are the zonal and meridional components of the geostrophic wind speed, respectively, Φ is the geopotential height value, f is Coriolis parameter, x is the zonal direction, and y is the meridional direction. According to the two components above, the geostrophic wind angle α_{g_ij} of the grid i, j can be calculated as follows:

$$\alpha_{g\_ij} = arctg\frac{u_{g\_ij}}{v_{g\_ij}} \tag{5}$$

where u_{g_ij} and v_{g_ij} represent the zonal and meridional components of the geostrophic wind speed.

To facilitate the subsequent computation, the geostrophic wind angle is mapped to the standard angle coordinate system in accordance with general meteorological regulations, by which north and east are set as 0° and 90°. For the grid points i, j, the geostrophic wind angle α_{g_ij} is calculated as:

$$\alpha_{g\_ij} = \begin{cases} arctg\frac{u_{g\_ij}}{v_{g\_ij}}, & u_{g\_ij} > 0; v_{g\_ij} > 0 \\ arctg\frac{u_{g\_ij}}{v_{ij}} + 2\pi, & u_{g\_ij} < 0; v_{g\_ij} > 0 \\ arctg\frac{u_{g\_ij}}{v_{ij}} + \pi, & u_{g\_ij} < 0; v_{g\_ij} < 0 \\ arctg\frac{u_{g\_ij}}{v_{g\_ij}} + \pi, & u_{g\_ij} > 0; v_{g\_ij} < 0 \end{cases} \tag{6}$$

To improve the accuracy of the curvature calculation, the bilinear interpolation method [16] is used to achieve α_{g1} and α_{g2} which are the geostrophic wind angles of two points before and after the current grid points, respectively, with a distance ΔL in the direction of the geostrophic wind (ΔL is far

less than the distance between the two grid points). Additionally, the curvature value C of the grid is calculated using central difference method as follows:

$$C = \frac{\partial \alpha_g}{\partial s_g} = \frac{\alpha_{g1} - \alpha_{g2}}{2\Delta L} \quad (7)$$

Thus, the curvature of each grid point is acquired via geopotential height field data rather than the complicated tracing process of contours.

2.2. Trough Line Analysis

For the geopotential height field, the trough line is connected by the points with the highest contour curvature in the low-pressure trough region. Therefore, the key to trough line analysis is to identify reasonable trough points for tracing and connecting based on the curvature value of grid points.

2.2.1. Curvature Comparison

Trough lines generally do not exhibit significant change in direction during their extension; therefore, directly tracing the local maximum curvature points to analyze trough lines may lead to large deflections in the tracing direction and unreasonable analysis results. Furthermore, extracting trough points based on a single curvature threshold is subject to the objective data attributes and subjective experience, which makes it difficult to determine an accurate and widely applicable threshold. However, when it comes to the manual analysis of trough lines, forecasters usually analyze the curvature of contours in a certain range comprehensively to select the grid points with larger curvature for connection to identify the trough line.

Thus, this study focuses on the locally relative magnitude of the curvature of grid points according to the above analysis. Therefore, a 3×3 matrix is established, centered at each grid point, as shown in Figure 1. In the figure, X is the center grid point, and the adjacent 8 grid points A~H serve as reference points for analyzing the relative magnitude of the curvature at point X. The curvature of point X is compared with its eight adjacent points to reflect the magnitude of the curvature at that point in the local range with N, which represents the number of adjacent points smaller than the curvature of X. If the N value is 8, then X is the point of maximum curvature in the local range. According to the definition of a trough line, if a trough line emerges within this range, then the point with the local maximum curvature should be one of the points in the trough line. In this way, the tracing starting point (the point whose N = 8) is determined and stored in the point set *StartPoint*.

A	B	C
H	X	D
G	F	E

Figure 1. Curvature comparison matrix.

2.2.2. Extraction of Candidate Trough Points

Actually, the discrete grid data contains a large number of grid points that should not be individually analyzed during trough line tracing due to the excessive noise and workload. Therefore,

prior to trough line tracing, the grid points are classified according to the magnitude of the curvature in the local range (N value) and their relative positions to extract the candidate trough points.

Normally, the trough line that passes through a certain grid point will also pass its two adjacent points, as shown in Figure 2a; that is, there exist at most two adjacent points (point A and E) with higher curvature than that of the grid point itself. Consequently, when N is no less than 6 for a grid point, that grid point will be designated as a candidate trough point.

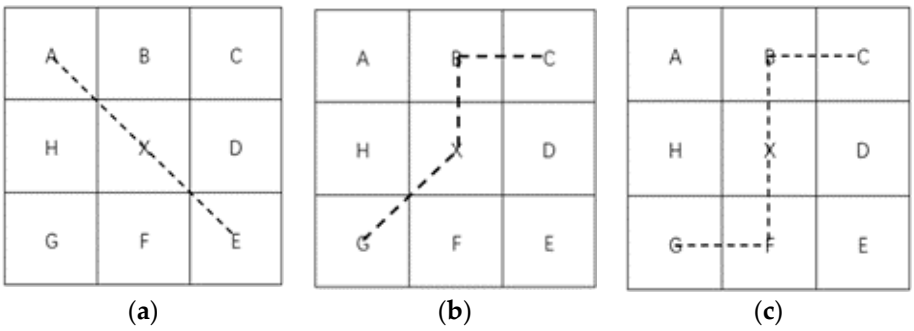

Figure 2. Trough point connection examples, the centre point X may has two (**a**) or three (**b**) or four (**c**) superior adjacent points in terms of the curvature value.

Furthermore, in the process of trough point tracing, if bending can be found at a grid point of a trough line, there may exist 3 or 4 adjacent points near the grid point X that have a larger curvature, as shown in Figure 2b,c. That is, the grid point with an N value of 4 or 5 is also essential for the correct tracing and connection of the trough lines. However, since most of the grid points with N = 4 or 5 are not located on the trough line as the results indicate, the determinant conditions should be set to further extract reasonable candidate trough points from these types of grid points.

Generally, no evident direction variation is found with reference to the extension of a trough line, and the extension direction is irreversible (no "U"-shaped backtracing allowed). Thus, the deflection angle of the trough line tracing direction is often less than 90°, and further extraction is carried out for the above grid points with $N < 6$:

(1) For grid points with N = 5, as shown in Figure 2b, assuming that there exist two superior adjacent points B and C, if the third point with a higher curvature is one of the points among E, F, G, and H (where the example just represents the relative position of grid points, below), the point X should be extracted as a candidate trough point.

(2) For grid points with N = 4, as shown in Figure 2c, assuming that two adjacent points B and C are found to have higher curvature, if another pair of adjacent points with higher curvature is E and F, F and G, or G and H, then the grid point X should also be extracted as a candidate trough point.

(3) For grid points with $N \leq 3$, the curvature is smaller at the localized points, which means the trough line would not pass through these types of grid points. Thus, we identify them as non-candidate trough points

To facilitate the identification, the candidates are represented using their N values, while "0" denotes the non-candidate trough points. Based on the 500 hPa geopotential height (150° E–155° E, 40° N–45° N) at 2200 UTC on 8 October 2013, the curvature calculation results are shown in Figure 3a. The extraction results are shown in Figure 3b, where the grid points with N = 8 imply the starting point of the trough line tracing and the remaining grid points with $N \neq 0$ are the candidate trough points.

4.8	8.0	11.9	16.3	17.8	15.1	13.9	13.4	8.9	3.9	3.0
6.1	8.9	12.4	17.1	17.8	13.0	10.3	11.2	10.5	6.8	5.2
8.1	10.3	13.9	19.2	17.7	10.1	7.3	8.0	7.4	5.5	4.9
10.7	12.7	16.7	20.9	17.1	8.9	5.2	4.0	2.6	1.5	1.7
12.9	15.5	19.6	21.0	14.8	7.2	3.2	1.2	0.0	-0.8	-0.7
14.8	17.5	19.0	15.9	9.7	5.2	2.7	1.0	-0.2	-1.1	-1.5
16.2	16.5	14.0	9.7	6.1	3.7	2.3	1.2	0.2	-0.6	-1.1
14.7	11.9	8.2	5.3	3.6	2.7	2.1	1.5	0.8	-0.1	-0.8
10.6	7.3	4.5	2.8	1.9	1.6	1.7	2.0	1.9	0.9	-0.6
7.4	5.0	2.9	1.5	0.8	0.6	1.0	2.0	3.0	2.7	1.0
5.8	3.9	1.9	0.6	0.1	0.0	0.3	1.4	3.0	3.9	3.1

(**a**)

0	0	0	0	5	0	0	0	0	0	0
0	0	0	0	7	0	0	6	6	0	4
0	0	0	7	5	0	0	0	0	0	0
0	0	0	7	0	0	0	0	0	0	0
0	0	6	8	0	0	0	0	0	0	0
0	6	6	0	0	0	0	0	0	0	0
6	6	0	0	0	0	0	0	0	0	0
5	0	0	0	0	0	0	0	0	0	0
0	0	0	0	0	0	4	5	0	0	0
0	0	0	0	0	0	0	6	6	0	0
0	0	0	0	0	0	0	0	6	8	0

(**b**)

Figure 3. Extraction of the tracing starting points and candidate trough points: (**a**) calculation results of the grid points' curvature. (**b**) The grid points marked by "8" imply the tracing starting points of the trough line and the other points with $N \neq 0$ represent the candidate trough points.

2.2.3. Trough Point Tracing

The trough point tracing process is initiated after the extraction of candidate trough points, and the reasonable trough points from the candidates are traced and connected from the starting point determined in Section 2.2.1. We firstly select the grid point with the largest curvature in the point set *StartPoint* as the tracing starting point of the first trough line, and the second largest as the next trough line and so forth. Meanwhile, the point set *MarkedPoint* is used to store the tracing starting points and the trough points have been traced.

According to the definition of the trough line, for grid points with a larger N value, the curvature is larger in the local range and is more likely to be located in the trough line. In addition, there exist no obvious direction change during trough point tracing. Based on the analysis above, we propose the rules for trough point tracing as follows:

(1) Preference for selecting the adjacent point around the current trough point with the largest N value (and $N \neq 0$) as the next trough point to trace.
(2) The adjacent point with the highest curvature is regarded as the next trough point when multiple adjacent points share the same maximum value of N.
(3) The deflection angle for tracing direction is no greater than 90°. As shown in Figure 1, if the previous tracing process is from A to X, then the next trough point should be selected from the five points C, D, E, F, and G.

Considering the tracing starting point is generally located at the middle position of the trough line, the tracing process for that trough line is never completed until the tracing on both the optimal and suboptimal directions from the starting point are finished. The conditions for completing the trough point tracing process are set as follows:

(1) According to the uncrossed rule of trough lines, the trough point tracing ends once a point in the set *MarkedPoint* has been traced again.
(2) If none of the adjacent points of the current trough point satisfies the tracing rules (stated above) for candidate trough points, the trough point tracing also ends.

All the trough line tracing starting points (those have been traced during an earlier tracing process are neglected) included in the *StartPoint* set are iterated in descending order of curvature. The raw trough line analysis results are completed with the above steps implemented repeatedly until all the starting points have been processed. For instance, the tracing result of the raw trough line at the 500 hPa

geopotential height (140° E–160° E, 30° N–50° N) at 2200 UTC on 8 October 2013 is shown in Figure 4, and the red box in the figure highlights the region shown in Figure 3.

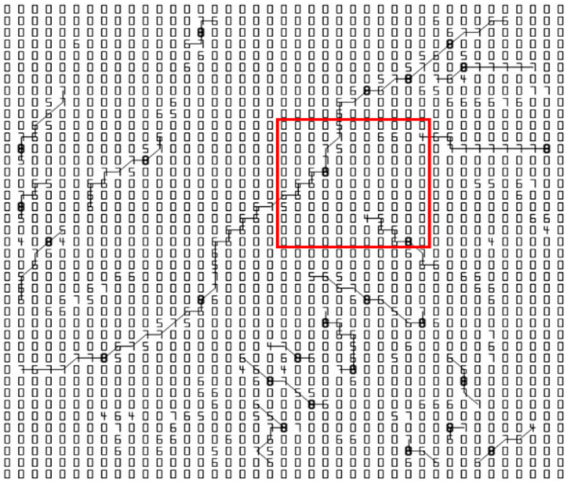

Figure 4. Tracing result of raw trough line using geopotential height field from 2200 UTC on 8 October 2013.

2.3. Post-Processing of Raw Trough Line

As a large-scale meteorological system, the wavelength of a trough line is usually quite long, and what forecasters ultimately need to be provided with are the smooth and noise-free results of trough line analysis. Therefore, after obtaining the raw trough lines through connecting and tracing trough points, some post-processing steps are still required to meet the demands of meteorological forecasting.

Firstly, the minimum length of a trough line is determined according to the resolution of the gridded data, which uses a *length threshold* parameter to filter out the short ones. By this mechanism, the main weather characteristics of that region can be reflected through the remaining large-scale trough lines, and a large number of false short troughs without practical significance can also be eliminated. Secondly, the *curvature threshold* is set to remove the trough lines that do not have analytical value (and is usually located in a region of relatively plain contour lines), saving the trough lines for which the curvature values of most of the trough points are greater than the threshold. Eventually, the B-spline curve function [17] is applied to achieve smooth trough lines, which serve as the final output of the automatic trough line analysis.

3. Results and Analysis

We implemented the proposed method on a computer and used geopotential height field from the European Center for Medium-Range Weather Forecasts (ECMWF) to test it. Section 3.2 demonstrates the case study results, and in Section 3.3, the proposed method was compared with some previous methods to validate the advantages of our method.

3.1. Data and Parameters

To examine the method proposed in this paper, the gridded data from ECMWF, which are widely applied in meteorologic fields and have significant linear correlation globally, were employed. ECMWF is also able to provide higher data accuracy [18] in comparison with some other types of gridded data, such as the data from the US National Center of Environmental Prediction (NCEP), and so on, which may be beneficial for improving the accuracy of automatic trough line analyses. The data includes the geopotential height value corresponding to latitude and longitude, and the data spatial resolution is $0.5^\circ \times 0.5^\circ$. In the field of meteorology, trough lines in regions such as the north and south poles, the area near equator, and the southern hemisphere are generally not the focus of analysis; thus, we set the experimental latitude

range as 70° N~20° N. In addition, the upper-level regional synoptic system has an important impact on the evolution of weather conditions, of which, it is known that 500 hPa geopotential height is a good diagnosis layer for deeper weather systems such as the westerly trough/ridge, the low-latitude subtropical high, and the polar vortex [19]. Therefore, we focused on the gridded data of the isobaric surface of 500 hPa to process the automatic analysis experiments of trough lines.

The method was mainly implemented through C# under the .NET framework. In terms of the method's parameters, the *length threshold* was set to 12, on the basis of the spatial data resolution of 0.5×0.5; additionally, the curvature of the trough points on the raw trough lines were accumulated to calculate the mean, which was set as the *curvature threshold* We decided that a trough line could be retained if more than two-thirds of its trough points' curvatures were greater than the curvature threshold.

3.2. Case Study Results

The post-processing of the raw trough line (shown in Figure 4) was performed according to the parameters set out in Section 3.1, whose results are shown in Figure 5. It can be seen that the final automatic analysis result is consistent with the distribution feature of the geopotential height field, and the trough line is smoother after curve fitting.

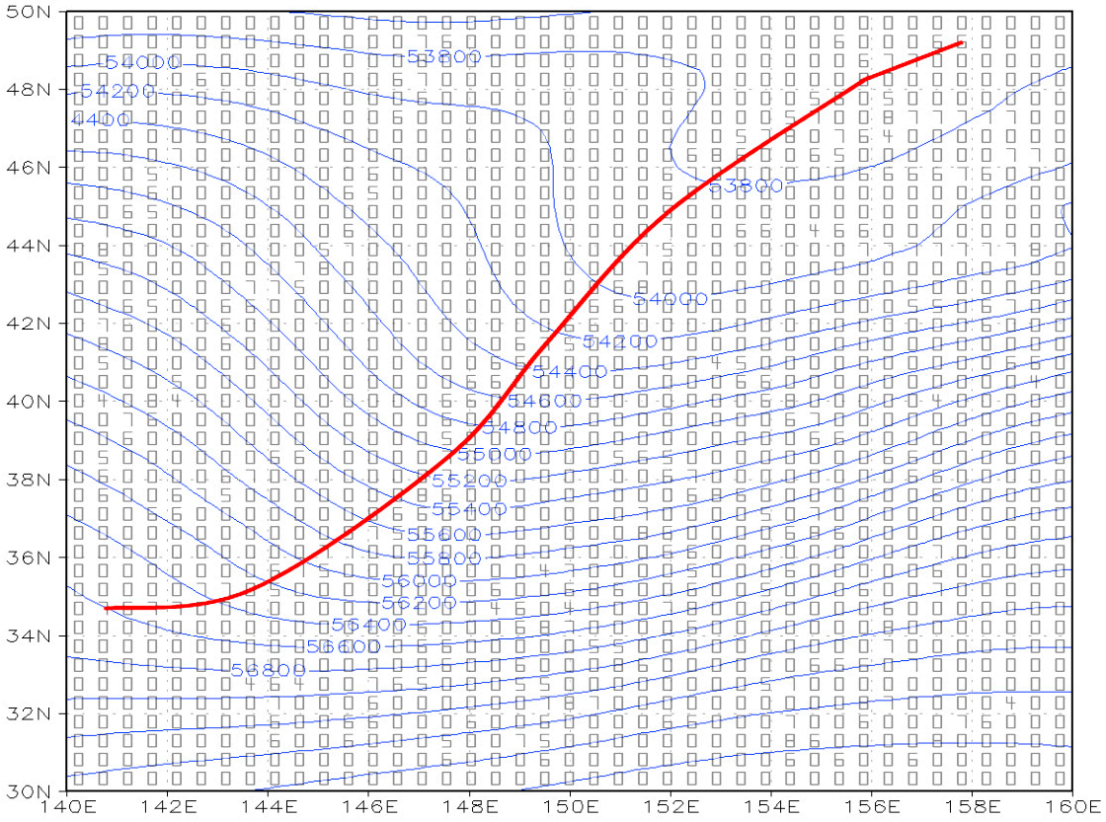

Figure 5. Post-processing result of trough line from 2200 UTC on 8 October 2013.

Furthermore, 24 sets of the geopotential height data at 500 hPa from March 2016 to February 2017 (two days from each month) were selected for trough line analysis batch experiments. Examples of the automatic analysis results are shown in Figure 6.

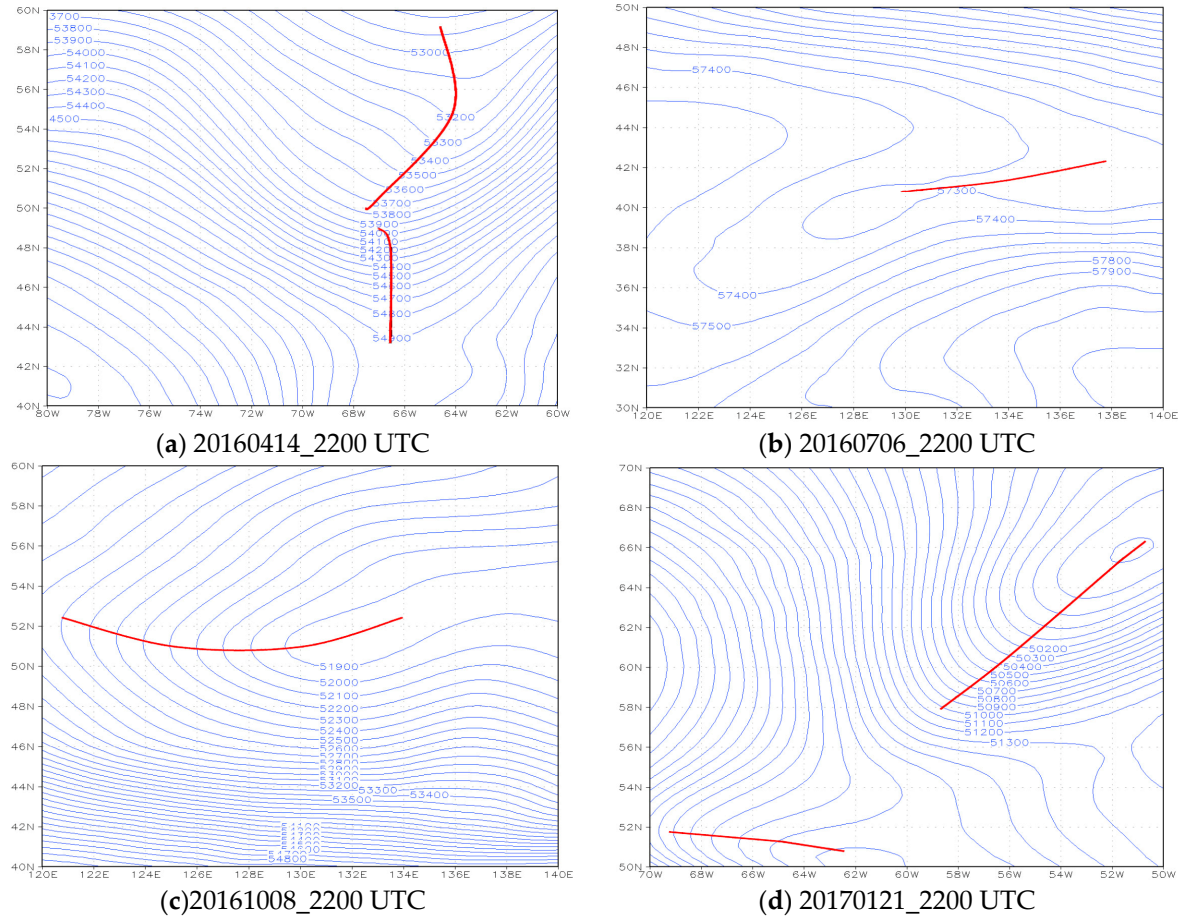

(**a**) 20160414_2200 UTC (**b**) 20160706_2200 UTC

(**c**)20161008_2200 UTC (**d**) 20170121_2200 UTC

Figure 6. (**a**–**d**) Automatic analysis results of trough line from 2200 UTC on 14 Apr 2016, 6 Jul 2016, 8 Oct 2016 and 21 Jan 2017. The examples were selected randomly from total automatic trough lines.

In the 24 sets of data used in the experiment, there were a total of 194 trough lines that were analyzed. To examine the accuracy of our method, two professional weather forecasters were invited to perform manual trough line analysis using the same geopotential height field data sets, and the analysis results were taken as the ground truth. We then delineated a small area around each manual trough line and identified whether a matching automatic trough line was located within the area of the manual trough line. If two trough lines formed a matching pair, then the qualitative evaluation method proposed in the previous research [20] was used. By calculating the consistency degree, the position consistency and scope consistency between two classes of trough lines in a matching pair were assessed:

$$\text{Consistency degree} = \left[\frac{N_{am}}{N_m + N_a - N_{am}}\right] \times 100 \tag{8}$$

In the equation, N_a and N_m represent the number of grid points in the automatic trough line and manual trough line respectively, and N_{am} is the number of grid points in both types of trough lines simultaneously. In particular, if the manual analyzed trough line passes between two grid points and at least one of these two points is located in the automatically analyzed trough line, we designate that a coincidence point (points in N_{am}) exists. The range of the consistency degree is from 0 to 100, and a greater degree indicates a greater similarity between two types of trough lines.

The consistency degree of all matching pairs from the geopotential height fields were calculated according to the above qualitative evaluation method, and the partial results (five matching pairs that were randomly selected from each data set, totaling 120 samples) are shown in Figure 7a. In addition, Figure 7b shows the number of matching pairs in each consistency degree range. In the figure, the orange

dotted line is the curve about the cumulative proportion of the number of matching pairs in different consistency degree intervals. It can be seen that the consistency degree of most matching pairs is in the range of 70–80, which indicates that the automatic trough lines are similar to the manual analysis results.

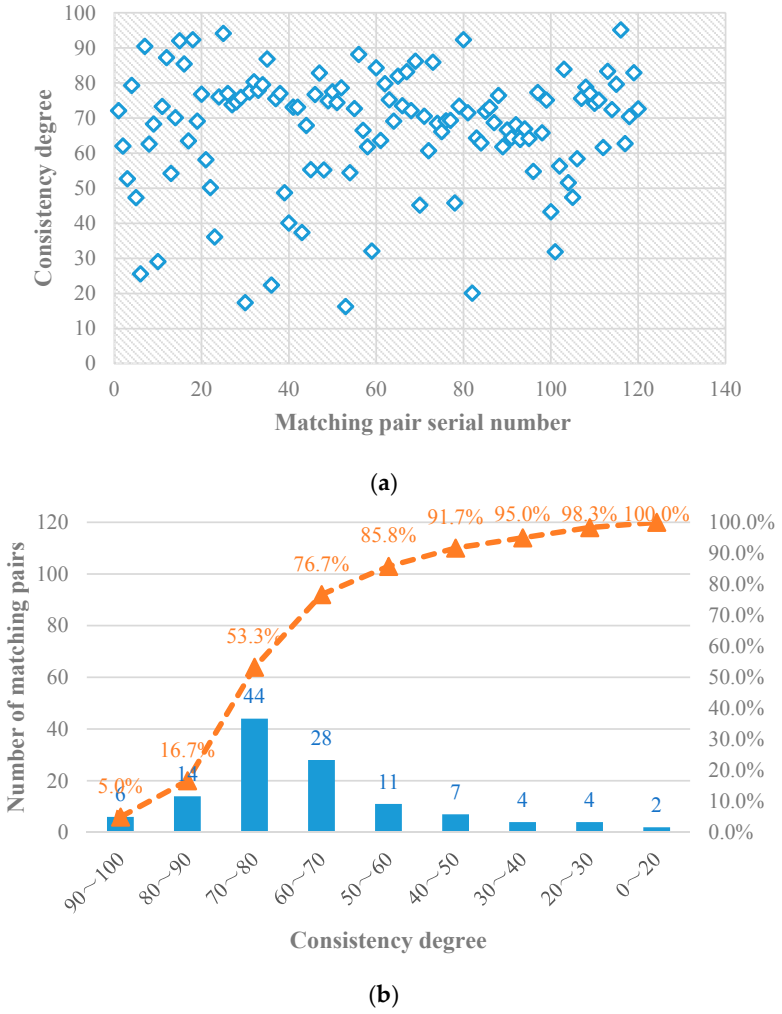

Figure 7. Computational (**a**) and statistical (**b**) results of the matching pairs' consistency degree, where the orange dotted line represents the curve with the cumulative proportion of the number of matching pairs in different consistency degree intervals

According to the professional forecasters, the automatic trough line analysis is considered a success if the matching pair's consistency degree is greater than 60, and from the Figure 7b, we find that at least 76.7% of the samples would have a consistency degree higher than 60. The statistical results of the trough line analysis are listed in Table 1, which are grouped by different seasons.

Table 1. Statistical results of the trough line analysis.

Season	Number of Manual Trough Lines	Number of Automatic Trough Lines	Number of Successfully Analyzed Trough Lines
Spring	39	44	32
Summer	30	36	23
Fall	51	54	45
Winter	57	60	51
Total	177	194	151

Thus, the evaluation indicators including recall ratio and precision ratio were defined to examine the validity and accuracy of our analysis method:

$$\begin{aligned} \text{Recall ratio} &= L_s / L_m \\ \text{Precision ratio} &= L_s / L_a \end{aligned} \tag{9}$$

where L_s is the number of successful matching pairs, L_m is the number of manual trough lines and L_a is the number of automatic trough lines.

The recall ratio and precision ratio obtained from the trough line analysis statistical results are shown in Figure 8. It can be seen that the total recall ratio and precision ratio reached 85.3% and 77.8%, respectively, which may meet the actual requirements for weather forecast. Moreover, we discovered that the automatic trough line analyses in the fall and winter were more effective and accurate than in the spring and summer. Further study reveals that high-altitude meteorological systems are more stable during the fall and winter seasons, making the trough line trend more obvious and located mostly in the region where the bending of the contours is relatively high (i.e., the change in curvature is significant), which may be easier for computers to analyze.

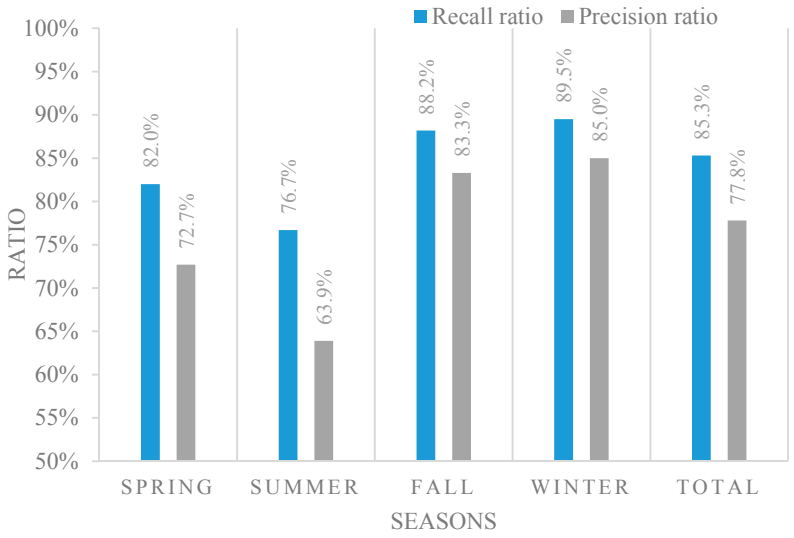

Figure 8. Recall ratio and precision ratio of automatically analyzed trough lines classified by seasons.

3.3. Comparison and Analysis

To validate the advantage of the proposed method, a comparative test was performed with some previous automatic analysis methods of trough lines. Among these, while the method proposed by Hu [9] can locate the approximate position of a trough and ridge meteorological system, it cannot extract the specific trough lines. Additionally, Wong's method [10] can only analyze the trough lines in the local region of interest. Therefore, the comparison is mainly made with ant colony theory-based [11], Douglas-Peucker algorithm-based [12] and principal curvature-based [14] methods. In the principal curvature-based method, the test data comprises two-dimensional gridded data, rather than three-dimensional. The four methods ([11,12,14] and our proposed method) were used to analyze trough lines based on the same gridded data from the batch experiments in Section 3.2, with the same computer; the results were assessed according to the qualitative evaluation method above, and the comparison results of recall ratio, precision ratio and processing time are shown in Figure 9. As shown in Figure 9a,b, our proposed method is better than the other three methods with regard to recall ratio and precision ratio overall; it is also more efficient, as shown in Figure 9c, in which the principal curvature-based method has the greatest time cost due to the necessity of some additional processing, such as curve approximation.

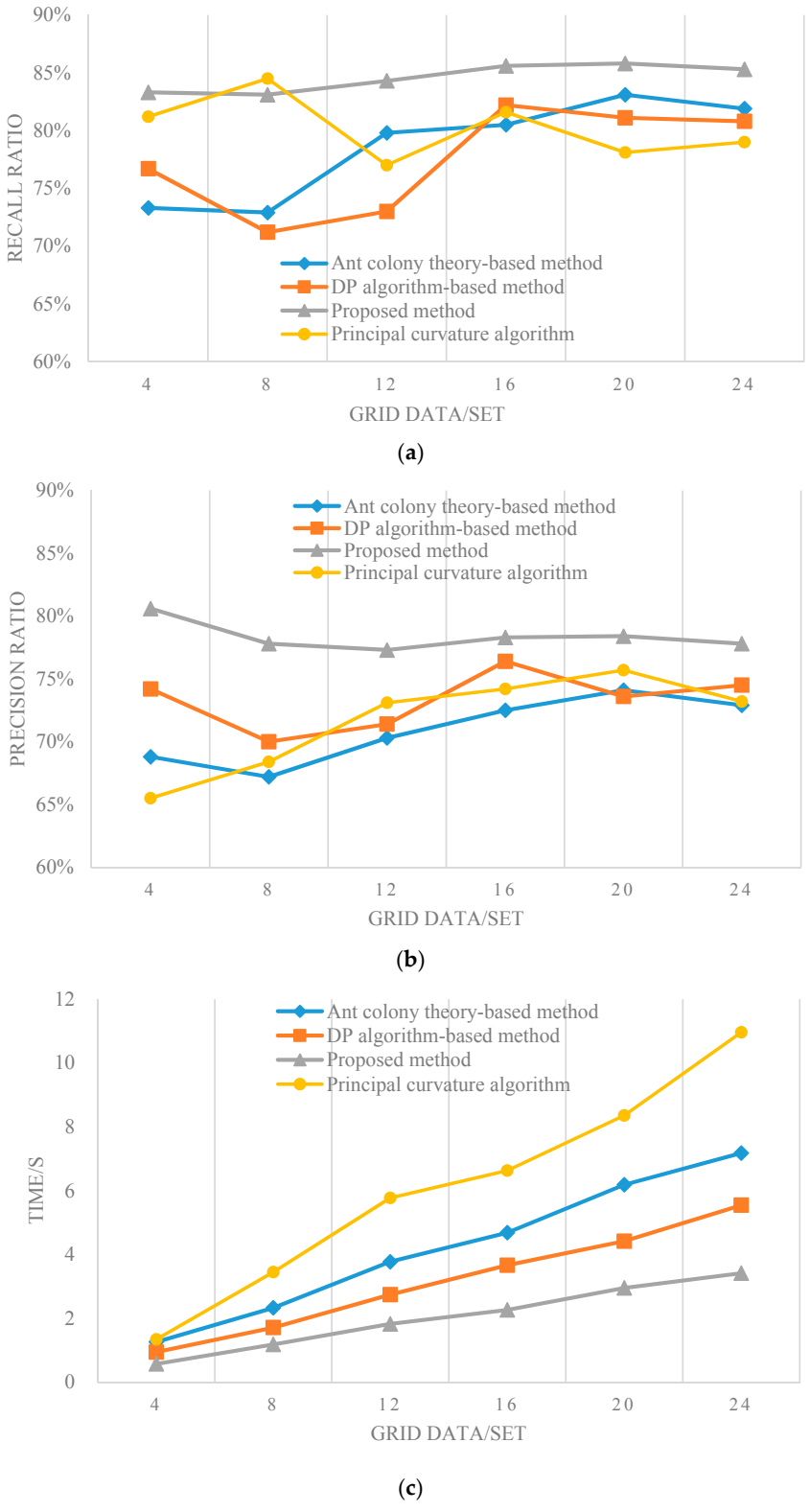

Figure 9. Comparison results of three different automatic analysis methods of trough lines in terms of recall ratio comparison (**a**), precision ratio comparison (**b**), and processing time comparison (**c**).

The average of three types of evaluation indicators of different methods were calculated, the results of which are shown in Table 2. It can be seen that the recall ratio of the proposed method is 8.6%, 11.0% and 6.3% higher than the ant colony theory-based, the DP algorithm-based and the principal

curvature-based automatic analysis methods, respectively. Furthermore, the proposed method improves the precision ratio by 11.4%, 7.6% and 8.6%, and shortens the processing time by 52.5%, 38.5% and 69% compared to the three other methods.

Table 2. Comparison results of the evaluation indicators of different automatic analysis methods of trough line.

Automatic Trough Line Analysis Method	Recall Ratio	Precision Ratio	Processing Time (s)
Proposed method	**85.31%**	**77.84%**	**0.142**
Ant colony theory-based	78.53%	69.85%	0.299
DP algorithm-based	76.83%	72.34%	0.231
Principal curvature-based	80.23%	71.68%	0.456

The above comparison test indicates that the proposed automatic analysis method based on curvature tracing is superior to the two previous methods in terms of recall ratio, precision ratio and processing time. Further study discovers that the ant colony theory-based method extracts trough lines mainly through interpolation data, which may easily introduce noisy data; moreover, the image edge detection algorithm used in the method may induce distortion when identifying the isobaric line sequence, thus affecting trough point extraction. Additionally, in the region where the contour lines are sparse, the method based on the DP algorithm may not satisfy the set of the distance factor due to the large distance between trough points, and thus will lead to the loss of some trough line analysis results in the region.

4. Conclusions

To improve the efficiency of trough line analysis for weather forecasting and to reduce the subjective uncertainty of manual analysis, this paper proposed an automatic method of trough line analysis based on curvature tracing. The method was primarily designed based on meteorological principles, and the curvatures of grid points were firstly calculated using geopotential height field data. Then, the starting points for tracing and candidate trough points were extracted according to their curvature and relative positions. Among the candidates, the eligible trough points were connected from the tracing starting points. Finally, the automatic analysis results of trough lines were recognized after some post-processing steps. The experimental results indicate that the method is able to identify meteorological trough lines effectively; furthermore, the automatic analysis results in the fall and winter were more accurate than in the spring and summer due to the different stabilities of the weather system. Compared to previous methods, our method is able to improve the efficiency and accuracy of trough line analysis with an average recall ratio of 85.31%, average precision ratio of 77.84% and average processing time of 0.142 s, which are superior to the other three methods. In general, our proposed method allows the automatic identification of trough lines with relatively high recall and precision ratios. Additionally, it can be applied in weather forecast practice.

However, the analysis results might be less accurate in areas with irregular geopotential height fields, which need more effort to improve. In addition, the self-adaptive method of the parameters set will be the focus in the future for robust results when it comes to different data resolutions.

Acknowledgments: We thank the editor and reviewers for their careful review and insightful comments. This paper was sponsored by the National Natural Science Foundation of China (No. 41305138 and No. 61473310) and the China Postdoctoral Science Foundation (No. 2017M621700).

Author Contributions: The work presented here was a collaboration between all authors. Qian Li outlined the method used and wrote the manuscript. Yan Huang performed the experiments. Yin Fan and Qian Li revised the manuscript. Shaoen Tang collected the related data information and proofed the manuscript. Yuntao Hu drew the figures and forms in the manuscript, he also contributed to checking spelling mistakes in the manuscript.

Conflicts of Interest: The authors declare no conflicts of interest.

References

1. Luo, B.; Tan, X.; Guo, Y. Introduction of MICAPS-A Chinese forecaster's interactive system. In Proceedings of the 86th AMS Annual Meeting/8th Conference on Atmospheric Chemistry, Atlanta, GA, USA, 27 January–3 February 2006; pp. 124–129.
2. Yufeng, T.; Kai, Q.; Xinke, Z.; Lijuan, Z. Meteorological graph web displaying based on the aggregation system. *Meteorol. Environ. Sci.* **2008**, *28*, 018.
3. Henry, R.K.; Welles, E.; Hopkins, T.; Brown-Leigh, O.; Tarro, A.M. AWIPS II overview and status. In Proceedings of the 25th Interactive Information and Processing Systems for Meteorology, Oceanography, and Hydrology, Phoenix, AZ, USA, 11–15 January 2009; Volume 37, pp. 805–813.
4. Ramamurthy, M.; James, M. AWIPS II in the university community. In Proceedings of the Unidata's efforts and capabilities of the software: EGU General Assembly Conference Abstracts, Vienna, Austria, 12–17 April 2015; pp. 734–741.
5. Walter, J. *Principles of Meteorological Analysis*, 4th ed.; The University of Chicago Press: Chicago, IL, USA, 1989; pp. 271–274.
6. Haase, H.; Bock, M.; Hergenröther, E.; Knöpfle, C.; Koppert, H.-J.; Schröder, F.; Trembilski, A.; Weidenhausen, J. Meteorology meets computer graphics—A look at a wide range of weather visualisations for diverse audiences. *Comput. Graph.* **2000**, *24*, 391–397. [CrossRef]
7. Huang, X.; Zhao, F. Relation-based aggregation: finding objects in large spatial datasets. *Intell. Data Anal.* **2000**, *4*, 129–147.
8. Huang, X. Automatic Analysis of Spatial Data Sets Using Visual Reasoning Techniques with an Application to Weather Data Analysis. Ph.D. Thesis, The Ohio State University, Columbus, OH, USA, 2000.
9. Hu, W.D.; Zhao, G.P.; Chen, X.G.; Li, Y.C.; Wang, C.W.; Shao, J. Auto-diagnosis on primary weather systems aloft and test on sandstorm. *J. Desert Res.* **2007**, *27*, 633–638.
10. Wong, K.Y.; Yip, C.L.; Li, P.W. Automatic identification of weather systems from numerical weather prediction data using genetic algorithm. *Expert Syst. Appl.* **2008**, *35*, 542–555. [CrossRef]
11. Mou, L.Y. *Research and Application of Trough Line Identification Based on Ant Colony System Theory*; Wuhan University of Technology: Wuhan, China, 2010.
12. Dai, X.; Li, Q.; Gu, D.Q. Automatic Recognition of Meteorological Trough Lines Based on Douglas-Peucker Algorithm. *Meteorol. Sci. Technol.* **2016**, *44*, 36–40.
13. Ohtake, Y.; Belyaev, A.; Seidel, H.P. Ridge-valley lines on meshes via implicit surface fitting. *ACM Trans. Graph.* **2004**, *23*, 609–612. [CrossRef]
14. Pang, X.F. An algorithm for extracting and enhancing valley-ridge features from point sets. *Acta Autom. Sin.* **2010**, *36*, 1073–1083. [CrossRef]
15. Phillips, N.A. Principles of Large Scale Numerical Weather Prediction. In *Dynamic Meteorology*; Springer: Berlin, Germany, 1973; Volume 11, pp. 294–298.
16. Kingston Daniel, M.S.; Anne Sophia, V.M.; Moses, C.J. A comparative analysis of bilinear based scalar algorithms. In Proceedings of the International 2014 International Conference on Circuit, Power and Computing Technologies, Nagercoil, India, 20–21 March 2014; pp. 1140–1145.
17. Wang, W.; Pottmann, H.; Liu, Y. Fitting B-spline curves to point clouds by curvature-based squared distance minimization. *ACM Trans. Graph.* **2006**, *25*, 214–238. [CrossRef]
18. Deng, X.H.; Zhai, P.M.; Yuan, C.H. Comparison and Analysis between Several Sets of Reanalysis Data. *Meteorol. Sci. Technol.* **2010**, *38*, 1–8.
19. Prichard, B. Synoptic analysis. *Weather* **2006**, *61*, 322. [CrossRef]
20. Gong, Y.; Li, J. The quantified verification method of synoptic meteorology and the application to AREM. *Sci. Meteorol. Sin.* **2010**, *30*, 763–772.

© 2018 by the authors. Licensee MDPI, Basel, Switzerland. This article is an open access article distributed under the terms and conditions of the Creative Commons Attribution (CC BY) license (http://creativecommons.org/licenses/by/4.0/).